

Fluorescent macrocyclic probes with pendant functional groups as markers of acidic organelles within live cells†

Cite this: *Org. Biomol. Chem.*, 2014, **12**, 823

Prashant D. Wadhavane,^a M. Ángeles Izquierdo,^a Dennis Lutters,^a M. Isabel Burguete,^a María J. Marín,^b David A. Russell,^b Francisco Galindo*^a and Santiago V. Luis*^a

A new family of acidity sensitive fluorescent macrocycles has been synthesized and fully characterized. Their photophysical properties including emission quantum yield and fluorescence lifetime have been determined. The acid–base properties of the new molecules can be tuned by the incorporation of pendant functional groups. The nature of such functional groups (carboxylic acid or ester) influences dramatically the p*K*_a of the probes, two compounds of which exhibit low values. Preliminary intracellular studies using confocal microscopy together with emission spectra of the probes from the cellular environment have shown that the synthesized fluorescent macrocycles mark the acidic organelles of RAW 264.7 macrophage cells.

Received 30th August 2013,
Accepted 13th November 2013

DOI: 10.1039/c3ob41773e

www.rsc.org/obc

Introduction

Fluorescence imaging of intracellular species is a field in continuous development.^{1–3} The number of molecules able to fluoresce selectively in the presence of specific species of interest such as cations, anions, radicals and neutral molecules has grown considerably over the last decades.^{4–9} Protons are perhaps the simplest analyte to target, but despite their simplicity the role that pH plays in the biological realm is of paramount importance.¹⁰ The concentration of protons determines the correct function of the cellular machinery, while unbalanced pH is linked to many diseased states. For instance, Alzheimer's disease, lysosomal storage diseases, renal tubular acidosis, diabetes, inflammation and cancer are disorders in which cellular pH lies far from the normal levels.¹¹ In many cases, the endosomal–lysosomal pathway (working at acidic pH, between 4 and 6) is malfunctioning, which implies a defective degradation of waste material, or an inadequate work of proton pumps in the membranes of the acidic organelles.¹²

A number of strategies have been followed in order to develop fluorescent pH probes for bioimaging of cellular components, in particular for acidic environments.^{13–18} Substitution at the fluorophore core with electron withdrawing substituents such as chloride and fluoride has been developed to lower the p*K*_a values of well-established near-neutral pH probes such as fluorescein and other xanthene derivatives.^{19,20} This strategy involves significant modifications of the synthetic procedures and, sometimes, unpredictable results of the final p*K*_a values of the resulting compounds. In addition, the substitution pattern of the fluorophore can often modify the absorption and emission properties, requiring a modification of the experimental protocols established for the imaging of the parent compounds.

A different strategy for designing fluorescent pH indicators for acidic organelles is based on the synthetic modification of anthrylmethylamines.^{21–26} The steric hindrance of the bulky and hydrophobic anthracene moiety contributes to the lower basicity of this family of pH sensors as compared to other amines containing smaller aromatic subunits or alkyl substituents. This characteristic makes them suitable for the measurement of pH in acidic environments and sets the basis for the development of, for example, the commercial LysoSensors DND-192 and DND-167. We have followed a similar strategy to develop a family of anthracene derivatives of pseudopeptidic nature.^{27,28} Structural modifications of 9,10-disubstituted anthracenes resulted in compounds exhibiting identical absorption and emission spectral parameters except for the fluorescent quantum yield, which is higher at acidic pH and

^aUniversitat Jaume I, Departamento de Química Inorgánica y Orgánica, Av. Sos Baynat, s/n, E-12071 Castelló de la Plana, Spain. E-mail: francisco.galindo@uji.es, luiss@uji.es; Tel: +34 964 72 8236

^bSchool of Chemistry, University of East Anglia, Norwich, Norfolk NR4 7TJ, UK. Tel: +44 (0)1603 593012

†Electronic supplementary information (ESI) available: ¹H and ¹³C NMR and mass spectra of compounds 1–4; absorption and emission spectra of compounds 1–4; fluorescence decay traces of compounds 1–4; distribution and fluorescence emission spectra of compounds 1 and 2 in RAW 264.7 macrophage cells. See DOI: 10.1039/c3ob41773e

depends on the chemical nature of the substituents. Biological experiments with RAW 264.7 macrophage cells and human monocytes demonstrated that the anthracene derivatives of pseudopeptidic nature could be used to study lysosomal structures within living cells by means of confocal fluorescence microscopy and flow cytometry.^{27,28} The work here presented reports on a further development of such a set of pseudopeptidic probes. The new compounds here described bear an additional pendant arm consisting of an acid or an ester group, which significantly modifies their acid–base properties, providing pH probes displaying lower pK_a values than related systems, and also enables future post-functionalization and modification of their solubility properties. The introduction of such functionalities is not trivial from the synthetic perspective. The synthesized anthracene derivatives have been chemically and photophysically characterized in solution and have been successfully tested as markers of acidic organelles in RAW 264.7 macrophage cells.

Results and discussion

Synthesis

Different pseudopeptidic macrocyclic structures containing an anthracene moiety have been reported previously by our group.^{27,28} An important example is the valine derivative **5** (Chart 1), which has been used as the reference molecule for this work. Variations in the macrocyclic architecture, such as the ring size or the nature of the side chain, have useful effects in the analytical performance of the macrocycles as fluorescent probes. Thus, it is possible to smoothly change the pK_a of the probes by 0.1–0.2 units, only by adding, for example, some strain to the macrocycle. This small effect could also be achieved by changing the hydrophobic character of the compound by varying the amino acid side chain. This *fine tuning* ability is of great interest in the area of sensor development since chemical changes performed with other probes can lead to drastic variations of the fluorescent properties (for instance in the fluorescein family of pH probes).^{19,20} Taking the fine tuning ability into account, macrocycles **1–4** (Chart 1) were designed and synthesized with a double objective: (1) to study the effect of a third nitrogen atom in the macrocyclic ring, and

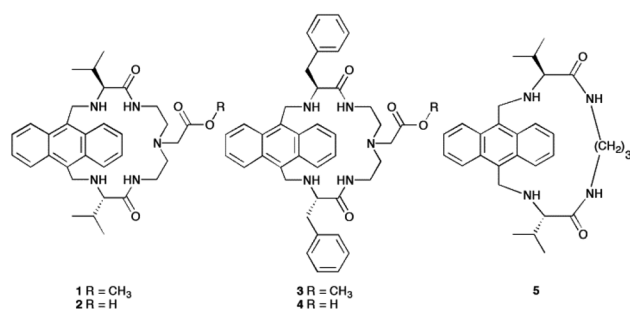
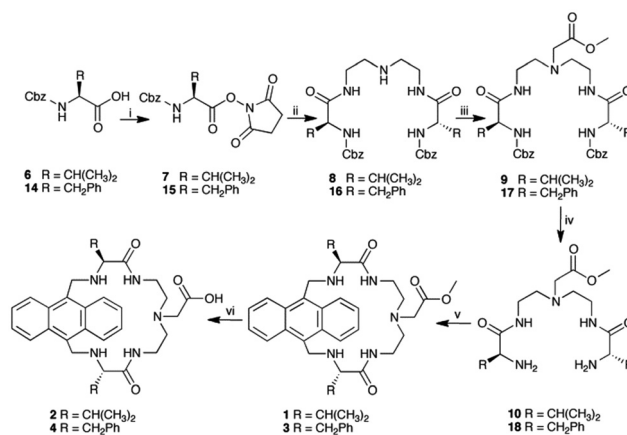


Chart 1 New anthracenophanes functionalized within the methylene bridge (**1–4**) and reference compound **5**.



Scheme 1 Synthesis of the anthracenophanes functionalized within the methylene bridge (**1–4**). Key: (i) DCC, *N*-hydroxysuccinimide, THF, rt, 6 h; (ii) NH₂(CH₂)₂NH(CH₂)₂NH₂, DME, 45 °C (18 h), rt (6 h); (iii) BrCH₂CO₂Me, K₂CO₃, dry DMF, 50 °C, 24 h; (iv) H₂/Pd, dry THF, 50 °C, 4 h; (v) 9,10-bis-(bromomethyl)-anthracene, K₂CO₃, CH₃CN, reflux, 24 h; and (vi) LiOH, 2 : 1 (v/v) H₂O–THF (2 : 1), rt, 24 h.

its substituents, on the basicity and solubility properties of the compounds; and (2) to evaluate their intracellular performance as fluorescent markers for acidic organelles in living cells using confocal fluorescence microscopy. Further, the new synthetic strategy herein reported allows the successful introduction of additional functional groups in the polymethylene bridge and sets the basis for the future development of new series of derivatives *via* anchoring other moieties or fluorophores.²⁹

Following a standard methodology developed in our group, compounds **1–4** were synthesized starting from the corresponding Cbz-protected amino acid (valine (Val) or phenylalanine (Phe)) which was activated at the C end by means of *N*-hydroxysuccinimide/*N,N*-dicyclohexylcarbodiimide (DCC) and further reacted with diethylenediamine to afford intermediates **8** and **16** (see Scheme 1). The central nitrogen of the bridge was then derivatized with methyl bromoacetate to afford intermediates **9** and **17** with good yields (75% and 76%, respectively). After deprotection of the Cbz groups the diamines **10** and **18** were obtained. These amines were reacted with 9,10-bis-(bromomethyl)-anthracene to afford the macrocyclic compounds **1** and **3** in 60–70% yield. Although moderate, these yields can be considered as an excellent result considering that no high dilution methods were employed. As we have previously studied,³⁰ the reason for such efficient macrocyclization could reside in the preorganized conformation of the reactive intermediates favoured by intramolecular hydrogen bonding and solvophobic effects, as well as by a kinetic template effect associated to the presence of halide anions.³¹ In the synthesis reported here, the presence of an alkylated nitrogen atom in the methylene bridge seems not to have a negative effect on the preorganization needed for the macrocyclization. Once the macrocycles with an ester pendant arm were obtained, the next step was the hydrolysis of these compounds with LiOH to yield the corresponding carboxylates. Isolation of

the compounds **2** and **4** required the utilization of exchange resins with a strong acidic character and final elution with an ammonia solution.³² The valine derivative **2** was obtained in a higher yield than the phenylalanine derivative **4**, probably due to the lower solubility of the more hydrophobic derivative **4** in the aqueous solvents needed for the ion exchange purification. At the end of the synthesis, several hundreds of milligrams of each macrocycle **1–4** were ready for chemical and photophysical characterization.

Characterization

Compounds **1–4** were characterized by means of Nuclear Magnetic Resonance spectroscopy (¹H and ¹³C NMR), Electro-Spray Ionization Mass Spectrometry (ESI-MS) and Fourier Transform Infrared Spectroscopy (FTIR) confirming the structures depicted in Chart 1. As described previously for other related systems, the ¹H NMR signals corresponding to the CH₂ at positions 9 and 10 of the anthracene moiety appear as two well defined doublets in the region located between 4.5 and 5 ppm, while the signal for the amide protons appear at 6.8 ppm for **1**, **2** and **4**; and 6.6 ppm for **3** (see ESI Fig. S4, S5, S9 and S10† for compounds **1–4**, respectively). These features constitute a characteristic landmark of this family of pseudopeptidic anthracene derivatives and indicate that the essential structural features are not affected by the introduction of a functionalized third nitrogen atom in the central spacer.

The UV-visible spectra of the macrocycles display the typical absorption of 9,10-disubstituted anthracene derivatives below 400 nm (see ESI Fig. S11A†). Thus, the presence of the pendant arms does not affect this feature; hence all of the spectra are almost identical and also match that of the reference compound **5**.

The fluorescence of the new macrocycles was recorded as a function of the acidity of the medium. Hence, pH titrations were conducted affording intensity variations as expected, *i.e.* strong emission at acidic values and low fluorescence in the neutral-alkaline environment (Fig. 1A). This phenomenon has been interpreted by the classical photoinduced-electron transfer (PET) mechanism extensively described in the literature.^{22–26,33–35} PET involves excitation of the anthracene moiety and fast quenching of the excited state by the neighbouring amines in their unprotonated form (in neutral-

Table 1 Photophysical features of compounds **1–4** and reference compound **5**

Probe ^a	λ_{abs} ^b (nm)	λ_{em} ^{b,c} (nm)	ϕ_{max} ^b	ϕ_{min} ^d	$\tau^{b,e}$ (ns)
1	359, 378, 400	405, 426, 450	0.75	0.017	13.3
2	359, 378, 398	404, 426, 451	0.73	0.010	13.0
3	359, 378, 400	405, 427, 451	0.77	0.031	13.7
4	359, 378, 400	405, 427, 453	0.78	0.020	13.3
5 ^f	358, 376, 397	405, 427, 453	0.77	0.009	13.0

^a Probe concentration (2 μM) in H₂O (0.2% DMSO). ^b Measured at pH 1.7. ^c $\lambda_{\text{exc}} = 374$ nm. ^d Measured at pH 8. ^e $\lambda_{\text{exc}} = 372$ nm, $\lambda_{\text{em}} = 420$ nm. ^f Data obtained from the literature.²⁸

alkaline media). Protonation of the amines results in the disruption of the PET and hence fluorescence enhancement in acidic media.

One of the striking features of the macrocycles described herein is the difference that exists between the *on* (fluorescent) and *off* (quenched) states, which is not commonly reported in the literature of pH sensors.^{36–41} The fluorescence quantum yields at pH 1.7 are in the range 0.73–0.78 whereas at pH 8.0 these values are substantially reduced to 0.010–0.031 (Table 1). This feature is ideal for obtaining microscopy images in which a *high contrast* between the bright (lower pH) and dark (high pH) areas of organelles within cells is desirable. The fluorescence emission spectra of the macrocycles **1–4** also exhibit the characteristic pattern of 9,10-disubstituted anthracene derivatives as shown in Fig. S11B.†

Time resolved fluorescence spectroscopy has also been used to characterize the singlet excited state of the new probes, providing emission lifetimes ranging between 13.0 and 13.7 ns (Table 1 and Fig. S12†). These values are in agreement with the one previously reported for the reference compound **5**, which indicates that the attachment of functionalities has no effect on the emission lifetime of the compounds.

From the pH fluorescence titrations, the intensity *vs.* pH profiles (Fig. 1B) were fitted to eqn (1) to calculate the corresponding pK_a values related to fluorescence quenching (Table 2). It should be noted that these pK_a values are related to the first deprotonation of one ammonium group located in proximity to the anthracene moiety, in the fully protonated macrocycle (polyammonium species). Once one of such amine is free, the electron pair located at that position is able to undergo PET and so quench the emission of the probe. Fig. 1B shows that there are two types of macrocycles according to the position of the titration curve: (1) those with the ester group as the pending functionality, with calculated pK_a values *ca.* 3.0–3.2; and (2) those probes with a carboxylic pending group, with calculated pK_a *ca.* 4.4–4.8. For comparison, the curve of the reference compound **5** (pK_a 5.06) has also been plotted in Fig. 1B.

$$\log \left(\frac{I_{\text{max}} - I}{I_{\text{min}} - I} \right) = \text{pH} - \text{pK}_a \quad (1)$$

Compounds **1** and **3** differ from the parent compound **5** in the number of amines of the macrocycle (considering that the

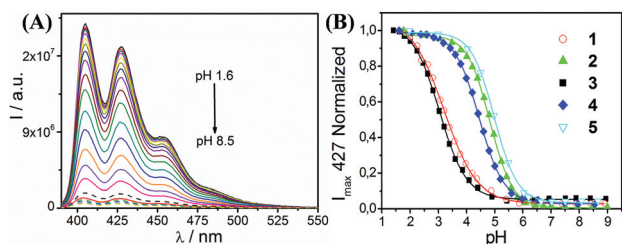


Fig. 1 (A) Fluorescence emission spectra of compound **3** as a function of the pH. (B) Fluorescence titration curves of compounds **1–4** and reference compound **5**. Experimental conditions: probe concentration (2 μM) in aqueous solution (0.2% DMSO); $\lambda_{\text{exc}} = 374$ nm.

Table 2 Calculated pK_a values for compounds 1–5 using the fluorescence titration curves and eqn (1)

Compound	pK_a
1	3.21
2	4.83
3	3.04
4	4.45
5 ^a	5.06

^a Data obtained from the literature.²⁸

ester group is playing a negligible effect on the acid–base equilibria). Hence, the differences between the calculated pK_a values (5.06 vs. 3.0–3.2) can be rationalized by considering that the new compounds are triamines whereas the reference is a diamine. It is well established in polyamine chemistry that the higher the number of amines in a system, the greater the difficulty to fully protonate the compound due to electrostatic repulsion between positive charges. This is particularly true when macrocyclic polyamines are considered, as the lack of conformational freedom makes the relaxation of this Coulombic repulsion difficult.⁴²

The hydrolysis of the ester group in 1 and 3 to yield molecules 2 and 4 has a dramatic effect on the pK_a of the resulting compounds. Thus, valine derivative 2 displays a pK_a of 4.83 in contrast with the pK_a of the related valine ester 1 (pK_a 3.21). The same effect was observed in 4 (pK_a 4.45) vs. 3 (pK_a 3.04). This effect is easily accounted for by charge neutralization due to the formation of a zwitterion (carboxylate-ammonium) in the central part of the bridge. This neutralization would render the pK_a of the macrocycles with the acidic functionality more similar to the pK_a of the reference compound 5 (pK_a 5.06) than to the pK_a of the probes 1 and 3, with the ester pendant group, *i.e.* behaving as a diamine rather than as triamines, in agreement with the behaviour reported in the literature for other compounds containing carboxylate or methylenephosphonate groups attached to the amino groups of polyazamacrocycles.⁴³

Cellular imaging using confocal microscopy

Once the basic photophysical and analytical features of the new compounds were established, their potential use as cell imaging probes was studied. Intracellular studies with compounds 1 and 2 were performed. Thus, a culture of RAW 264.7 macrophage cells was incubated with these compounds and simultaneously with the marker of acidic organelles LysoSensor Green DND-189. The tested molecules were readily uptaken by the cells, possibly *via* a plasma membrane carrier, with consideration of their polyamine nature, as previous examples described in the literature.⁴⁴ The images in Fig. 2 show that the fluorescence from the blue channel (corresponding to the emission of the anthracene, Fig. 2A and 2D) and from the green channel (fluorescence due to the LysoSensor Green DND-189, Fig. 2B and 2E) appear to co-locate. The same pattern was observed repeatedly in a number of cells (see

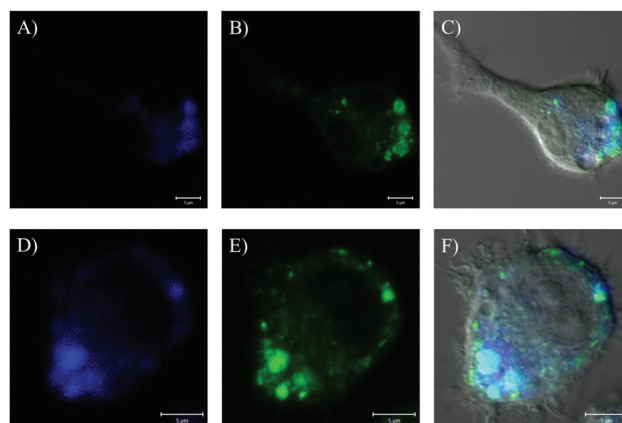


Fig. 2 Distribution and colocalization experiments with probes 1 and 2 and LysoSensor Green DND-189 in RAW 264.7 macrophage cells. (A) Fluorescence image of the compound 1, collected with a confocal laser scanning microscope in the blue channel. (B) Fluorescence image of the DND-189 probe collected with a confocal laser scanning microscope in the green channel. (C) Composite images of blue, green and DIC channels for compound 1. (D) Fluorescence image of the compound 2, collected with a confocal laser scanning microscope in the blue channel. (E) Fluorescence image of the DND-189 probe collected with a confocal laser scanning microscope in the green channel. (F) Composite images of blue, green and DIC channels for compound 2.

ESI†). These experiments confirm that probes 1 and 2 act as markers of the acidic organelles within RAW 264.7 macrophage cells.

A final experiment was performed in order to confirm that the fluorescence emission observed in the blue channel corresponds to the anthracene fluorophore and not to autofluorescence from the components of the cellular environment. Autofluorescence of the cells can lead to significant emission when the cells are excited with UV light. To discriminate the autofluorescence of the cells from the fluorescence due to the molecular probe, the fluorescence emission spectra of the areas *inside* the cell with higher fluorescence intensity were recorded. The shape and position of the spectrum recorded within the cell was compared to the spectrum of 2 recorded in solution. This strategy has been recently applied to study the nature of the intracellular reaction products of 1,2-diamino-anthraquinone (a fluorescent probe for nitric oxide).⁴⁵ Also, the measurement of intracellular spectra has been of great utility to calculate the pH of localized areas within Chinese hamster ovary (CHO) cells using a gold nanoparticle based fluorescent sensor.^{46,47} Fig. 3A–C show a RAW 264.7 macrophage cell incubated with 2 that displays areas of strong fluorescence emission when excited with a 364 nm UV laser. The fluorescence emission spectra of three areas within the bright spot reveal clearly the anthracenic origin of the emission (Fig. 3D, areas 1–3). Control experiments were performed recording spectra of darker zones (see Fig. 3D, areas 4–6). More examples of fluorescence emission spectra recorded from within RAW 264.7 macrophage cells incubated with probe 2 are given in Fig. S15.† The same study was carried out for probe 1 and analogous results were obtained (see ESI Fig. S16 and S17†).

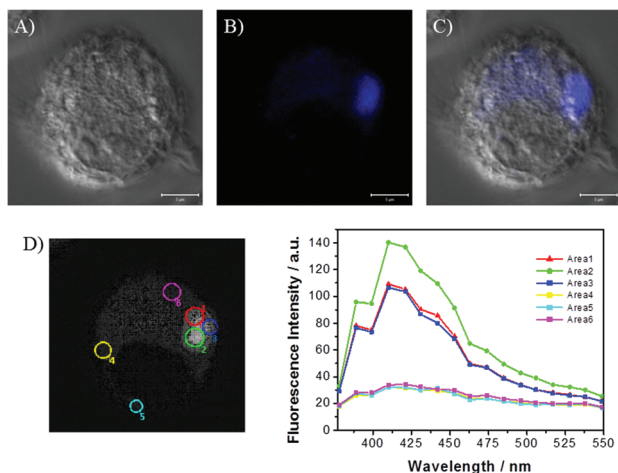


Fig. 3 Intracellular emission spectra of probe 2. (A) DIC image was collected with a confocal laser scanning microscope in the DIC mode. (B) Fluorescence image of 2 was collected with a confocal laser scanning microscope in the blue channel. (C) Composite image of blue and DIC channels. (D) Fluorescence emission spectra of compound 2 inside the cells selecting different areas within the cells.

Conclusions

Four new fluorescent macrocycles with high structural complexity have been synthesized, characterized and their photophysical properties, including emission quantum yields and fluorescence lifetimes, have been determined. The sensitivity towards pH has been studied, with calculation of the pK_a values of the new probes. Preliminary intracellular studies using RAW 264.7 macrophage cells have demonstrated that the new macrocycles can be used as markers of acidic organelles, as demonstrated by colocalization with a known lysosomal probe. Additionally, the fluorescence emission spectra, recorded directly from within the live cells, have confirmed the identity of the probe responsible for the fluorescence. Of important significance is the fact that the introduction of an ester group as a pendant arm far from the fluorescent moiety has led to a dramatic shift of the apparent pK_a of the probe towards acidic pH.

Experimental section

Chemicals and starting materials

The solvents and reagents were used as received, without further purification. 9,10-Bis(bromomethyl)-anthracene was synthesized using a procedure described in the literature.²⁷ Compounds 7 and 15 were synthesized using a procedure developed in our group and were obtained with similar yields.³⁰

Methods and techniques

NMR spectroscopy. ^1H and ^{13}C NMR spectra were recorded on a 500 MHz spectrometer (500 MHz for ^1H and 125 MHz for ^{13}C) or a 300 MHz spectrometer (300 MHz for ^1H and 75 MHz

for ^{13}C). Chemical shifts for all the compounds are reported in ppm (δ).

Mass spectrometry. Mass spectra were recorded on a hybrid QTOF I (quadrupole–hexapole–TOP) mass spectrometer with an orthogonal Z-spray-electrospray interface. Nitrogen was used as the desolvation and the nebulizing gas at a flow of 700 L h^{-1} and 20 L h^{-1} , respectively. The temperature of the source block was set to $120\text{ }^\circ\text{C}$ and the desolvation temperature to $150\text{ }^\circ\text{C}$. A capillary voltage of 3.5 and 3.3 kV was used in the positive and negative scan mode, respectively. The cone voltage was typically set to 20 V to control the extent of fragmentation of the identified ions. Sample solutions were infused *via* a syringe pump directly connected to the SI source at a flow rate of 10 L min^{-1} . The observed isotopic pattern of each intermediate matched perfectly to the theoretical isotope pattern calculated from their elemental composition equipped with an electrospray ionization source and a triple-quadrupole analyzer.

UV-Vis experiments. UV-visible absorption measurements were made using a UV-visible spectrophotometer. All samples were measured in aerated conditions unless otherwise stated.

Steady-state fluorescence spectroscopy. Steady-state fluorescence spectra were recorded with a Spex Fluorog 3-11 equipped with a 450 W xenon lamp. Fluorescence spectra were recorded in the front face mode. The samples were measured in aerated conditions, unless otherwise stated.

Time-resolved fluorescence spectroscopy. Time-resolved fluorescence measurements were performed using the technique of time correlated single photon counting (TCSPC) in an IBH-5000U. The samples were excited using a 372 nm NanoLED with a FWHM of 1.3 ns at repetition rate of 100 kHz. Data were fitted to the appropriate exponential model after deconvolution of the instrument response function by an iterative deconvolution technique, where reduced χ^2 and weighted residuals serve as parameters for the goodness of fit. The samples were measured in aerated conditions, unless otherwise stated.

Sample preparation for photophysical characterization. Stock solutions of compounds 1–4 (1 mM) were prepared in DMSO. The stock solutions were diluted in H_2O to a final concentration of $2\text{ }\mu\text{M}$. The pH of the diluted solutions was adjusted by adding aliquots of HCl and NaOH at different concentrations.

Fluorescence quantum yield measurements. Fluorescence quantum yields (ϕ_s) of compounds 1–4 in water, upon excitation at 372 nm, were reported relative to 5 ($\phi_r = 0.77$).²⁸ The experiments were performed using optically matched solutions and the quantum yields were calculated using eqn (2),

$$\phi_s = \phi_r \frac{A_r F_s \eta_s^2}{A_s F_r \eta_r^2} \quad (2)$$

where A_s and A_r are the absorbance of the sample and reference solutions, respectively, at the same excitation wavelength; F_s and F_r are the corresponding relative integrated fluorescence intensities of the sample and the reference; and η_s and η_r are

the refractive indexes of the solvent used to measure the sample and the reference.

Intracellular studies

Imaging medium. Imaging medium was prepared in analytical reagent grade water containing sodium chloride (120 mM), potassium chloride (5 mM), calcium chloride (2 mM), magnesium chloride (1 mM), sodium dihydrogen phosphate (1 mM), sodium hydrogen carbonate (1 mM) and 4-(2-hydroxyethyl)piperazine-1-ethanesulfonic acid (HEPES, 25 mM). The pH of the imaging medium was adjusted to pH 7.2. The imaging medium was supplemented with bovine serum albumin (1 mg mL⁻¹), basal medium Eagle amino acid (2%), glutamine (2 mM) and glucose (11 mM). The imaging medium was sterilized by filtration through a Millex® GP syringe driven filter unit (0.22 µm) prior to use.

Cell culture. The mouse macrophage cell line RAW 264.7 was cultured in Dulbecco's Modified Eagle's Medium (1×) containing 4.5 g L⁻¹ D-glucose (DMEM) supplemented with 1% L-glutamine (200 mM), 1% penicillin–streptomycin (100 U mL⁻¹ and 100 µg mL⁻¹, respectively) and 10% fetal calf serum. The cells were grown at 37 °C in a 7.5% CO₂ atmosphere in Nunc Easy flasks with porous caps. Subcultures (1:3) were made every 3 days by dislodging the cells from the flask surface using a cell scraper. For imaging, RAW 264.7 macrophage cells were cultured on 18 mm diameter glass coverslips a day prior to performing the imaging experiments. Cells were harvested from the Nunc Easy flask using a cell scraper and placed on a sterile coverslip in each well of a 6-well Nunc multidish. The cells were cultured in supplemented DMEM at 37 °C in a 7.5% CO₂ atmosphere overnight.

Incubation of RAW 264.7 macrophage cells with 1 or 2. The RAW 264.7 macrophage cells were loaded with **1** (50 µM, 0.5% DMSO) or **2** (50 µM, 0.5% DMSO) and incubated at 37 °C in a 7.5% CO₂ environment for 20 min. Stock solutions of compounds **1** and **2** (10 mM in DMSO) were used to load the cells.

Incubation of RAW 264.7 macrophage cells with 1 or 2 and LysoSensor Green DND-189. After incubating the RAW 264.7 macrophage cells with compound **1** or **2** for 20 min, LysoSensor Green DND-189 (2 µM, 0.2% DMSO) was added to the cells. The cells were incubated at 37 °C in a 7.5% CO₂ atmosphere for 5 min.

Imaging of RAW 264.7 macrophage cells loaded with 1 or 2. For imaging, 18 mm coverslips containing the RAW 264.7 macrophage cells were placed in a Ludin chamber (Life Imaging Service, Olten, Switzerland) which was securely tightened. The cells on the coverslip were washed three times with the imaging medium and the Ludin chamber was mounted on a heating stage at 37 °C in a Carl Zeiss LSM510 META confocal laser scanning microscope. The images were acquired with a Plan-Neofluar ×40, a 1.3NA oil immersion objective. The cells were excited with a 364 nm UV laser and the fluorescence emission was collected above 385 nm. Differential interference contrast (DIC) images were collected simultaneously using a 488 nm argon-ion laser. The fluorescence emission spectra of the samples were obtained using a lambda scan mode

between 378 and 549 nm exciting the sample with a 364 nm UV laser. The fluorescence emission intensity was measured in spectral bands each of 10.8 nm width. Images and spectra were processed using the Zeiss LSM Image Browser Version 4.2.0.121 software.

Imaging of RAW 264.7 macrophage cells loaded with 1 or 2 and LysoSensor Green DND-189. Imaging of RAW 264.7 macrophage cells loaded with both the compounds **1** or **2** and the LysoSensor Green DND-189 was achieved by exciting the cells at two different wavelengths. As previously described, the cells were excited with a 364 nm UV laser to collect the emission from **1** or **2**. The fluorescence emission was collected between 383 and 447 nm (blue channel). To collect the fluorescence emission due to the LysoSensor Green DND-189, the cells were excited with a 488 nm argon-ion laser and the fluorescence emission was collected between 505 and 550 nm (green channel). DIC images were collected simultaneously using a 488 nm argon-ion laser.

Synthesis and characterization of organic compounds

Synthesis of 8. To a clear solution of the *N*-hydroxysuccinimide ester of *N*-Cbz-L-valine **7** (30.0 g, 86.12 mmol) in anhydrous dimethoxyethane (DME, 250 mL) at 0 °C, diethylenetriamine (4.46 g, 43.06 mmol) dissolved in dry DME (20 mL) was added in a dropwise manner. The reaction mixture was stirred at room temperature for 18 h and then was heated to 40–50 °C for 6 h. The white solid formed was filtered and washed with cold water and cold methanol (23.27 g, 0.04 mol, 94% yield): mp 175–176 °C; $[\alpha]_{\text{D}}^{25} = 11.39^\circ$ (*c* 0.1, CHCl₃); IR (ATR) 3285, 2957, 1685, 1649, 1535 cm⁻¹; ¹H NMR (500 MHz, DMSO-*d*₆) δ 7.83 (s, 2H), 7.38–7.19 (m, 12H), 5.03 (s, 4H), 3.79 (m, 2H), 3.10 (dd, 4H, *J* = 12.6, 6.1 Hz), 2.51 (m, 4H), 1.92 (m, 2H), 0.83 (d, 12H, *J* = 6.1 Hz); ¹³C NMR (75 MHz, DMSO-*d*₆) δ 174.9, 171.8, 156.8, 137.8, 128.9, 128.3, 66.1, 61.1, 48.9, 30.9, 25.7, 19.9, 18.9; HRMS (ESI-TOF)⁺ (*m/z*) calcd for C₃₀H₄₃N₅O₆ (M + H⁺) 570.3292, found 570.3296. Anal. calcd for C₃₀H₄₃N₅O₆ H₂O: C, 61.3; H, 7.7; N, 11.9. Found: C, 61.4; H, 7.8; N, 11.9.

Synthesis of 9. A mixture of compound **8** (10 g, 17.55 mmol), anhydrous K₂CO₃ (24.25 g, 175.5 mmol) and methyl bromoacetate (2.68 g, 19.30 mmol) was placed in a flask containing dry dimethylformamide (DMF, 10 mL) and heated to 50 °C for 24 h under a nitrogen atmosphere. The reaction was monitored by TLC. After complete consumption of the starting material, distilled water was added (30 mL). This solution was extracted by using ethyl acetate (EtOAc, 30 mL, ×3). The organic phase was dried over anhydrous MgSO₄ and evaporated under vacuum. The product was purified by silica flash chromatography using MeOH–CH₂Cl₂ (1:50) to give the white solid **9** (8.19 g, 12.80 mmol, 75% yield): mp 156–158 °C; $[\alpha]_{\text{D}}^{25} = -10.45^\circ$ (*c* 0.1, CHCl₃); IR (ATR) 3300, 3064, 3031, 2949, 2869, 2360, 1736, 1685, 1644, 1532 cm⁻¹; ¹H NMR (500 MHz, DMSO-*d*₆) δ 7.77 (s, 2H), 7.39–7.24 (m, 10H), 7.17 (d, 2H, *J* = 8.8 Hz), 5.00 (m, 4H), 3.78 (t, 2H, *J* = 7.9 Hz), 3.58 (s, 3H), 3.37 (d, 2H), 3.10 (m, 4H), 2.63 (m, 4H), 1.91 (m, 4H), 0.82 (m, 12H); ¹³C NMR (126 MHz, CDCl₃) δ 173.73, 171.50, 139.76, 129.31, 128.59, 127.47, 67.53,

55.69, 54.98, 53.56, 51.53, 37.45, 31.24, 19.49, 17.96; HRMS (ESI-TOF)⁺ (*m/z*) calcd for C₃₃H₄₇N₅O₈ (M + H⁺) 642.3503, found 642.3508. Anal. calcd for C₃₃H₄₇N₅O₈: C, 61.8; H, 7.4; N, 10.9. Found: C, 61.7; H, 7.5; N, 10.9.

Synthesis of 10. To a clear solution of compound **9** (2.00 g, 3.11 mmol) in dry tetrahydrofuran (THF), 10 mol% of the catalyst (5 wt% Pd on activated carbon) was added. The reaction mixture was stirred under an atmosphere of H₂ (H₂ balloon) at 50 °C for 4 h. The reaction was monitored by TLC, and after complete consumption of the starting material the catalyst was filtered off through a Celite® bed and washed with THF. The crude product was purified by column chromatography using MeOH–CH₂Cl₂ (1 : 15) as an eluent, to which NH₃ (20 μL) was also added at every addition of the eluent throughout the column. Evaporation of the solvent under vacuum yielded the green oil **10** (0.462 g, 1.24 mmol, 80% yield): [α]_D²⁵ = 6.26° (*c* 0.1, CHCl₃); IR (ATR) 3289, 3073, 2963, 2869, 1736, 1640, 1526 cm⁻¹; ¹H NMR (500 MHz, CDCl₃) δ 7.50 (s, 2H), 3.26 (m, 4H), 3.09 (m, 2H), 2.66 (m, 4H), 2.10 (m, 2H), 1.59 (m, 5H), 0.87 (d, 6H, *J* = 6.8 Hz), 0.74 (d, 6H, *J* = 6.8 Hz); ¹³C NMR (75 MHz, CDCl₃) δ 174.3, 171.8, 68.2, 54.8, 54.1, 51.0, 43.4, 36.9, 31.2, 19.6, 17.9, 15.2; HRMS (ESI-TOF)⁺ (*m/z*) calcd for C₁₇H₃₅N₅O₄ (M + H⁺) 374.2767, found 374.2762. Anal. calcd for C₁₇H₃₅N₅O₄: C, 49.9; H, 9.6; N, 17.1. Found: C, 49.9; H, 9.7; N, 17.0.

Synthesis of 1. A mixture of compound **10** (0.50 g, 1.33 mmol), anhydrous K₂CO₃ (1.85 g, 13.38 mmol) and 9,10-bis(bromomethyl)-anthracene (0.54 g, 1.47 mmol) in dry CH₃CN (175 mL) was stirred till reflux for 24 h under a nitrogen atmosphere. The reaction was monitored by TLC. After complete consumption of the starting material, the reaction mixture was filtered and the solvent was evaporated under vacuum. The crude product was purified by silica flash chromatography using MeOH–CH₂Cl₂ (1 : 25) as the eluent to yield the yellowish solid compound **1** (0.542 g, 0.942 mmol, 70% yield): mp 94–95 °C; [α]_D²⁵ = –51.30° (*c* 0.1, CHCl₃); IR (ATR) 3329, 2950, 2920, 2861, 1746, 1661, 1590 cm⁻¹; ¹H NMR (500 MHz, DMSO-*d*₆) δ 8.57 (m, 4H), 7.65 (m, 4H), 6.87 (s, 2H), 5.01 (d, 2H, *J* = 13.9 Hz), 4.72 (d, 2H, *J* = 13.8 Hz), 3.55 (s, 3H), 3.11 (m, 4H), 2.70 (s, 2H), 2.19–1.99 (m, 6H), 1.92 (m, 2H), 1.06 (d, 6H, *J* = 6.3 Hz), 0.89 (d, 6H, *J* = 6.9 Hz); ¹³C NMR (126 MHz, CDCl₃) δ 173.2, 171.7, 132.9, 129.9, 125.8, 125.6, 68.7, 52.9, 52.6, 51.2, 45.1, 36.8, 31.2, 19.8, 18.2; HRMS (ESI-TOF)⁺ (*m/z*) calcd for C₃₃H₄₅N₅O₄ (M + H⁺) 576.3550, found 576.3557. Anal. calcd for C₃₃H₄₅N₅O₄: C, 66.8; H, 7.9; N, 12.2. Found: C, 66.6; H, 7.7; N, 12.2.

Synthesis of 2. To a clear solution of **1** (0.3 g, 0.52 mmol) in 6 mL THF–H₂O (2 : 1), LiOH (0.087 g, 3.64 mmol) was added and the reaction was stirred at room temperature for 24 h. The reaction was monitored by TLC and, after complete consumption of the starting material, the reaction mixture was made acidic (pH 6) with 1 : 1 HBr–H₂O. This solution was added to the washed DOWEX® ion exchange resin (4 g), and then left for 18 h at room temperature. The solvent of this mixture was evaporated under vacuum, and then the resulting solid was added to a column containing 20 g washed DOWEX® ion

exchange resin and deionized H₂O. The eluents used for the resin column purification were: H₂O (100 mL), 1 : 1 THF–H₂O (100 mL), 5% NH₃ in H₂O and then, 10% NH₃ in H₂O. The compound was isolated in the range of 5–10% NH₃ in H₂O solutions. Then the water was evaporated under vacuum to yield the yellowish solid **2** (0.103 g, 0.182 mmol, 35% yield): mp 105–107 °C; [α]_D²⁵ = –85.25 (*c* 0.1, CHCl₃); IR (ATR) 3428, 3149, 2965, 2871, 1651, 1568 cm⁻¹; ¹H NMR (500 MHz, DMSO-*d*₆) δ 8.44 (m, 4H), 7.52 (m, 4H), 6.76 (s, 2H), 4.88 (d, 2H, *J* = 13.9 Hz), 4.60 (d, 2H, *J* = 13.7 Hz), 2.98 (m, 2H, *J* = 4.6 Hz), 2.84 (s, 2H), 2.00 (m, 6H), 1.80 (m, 2H), 0.94 (d, 6H, *J* = 6.9 Hz), 0.74 (d, 6H, *J* = 6.9 Hz); ¹³C NMR (126 MHz, DMSO-*d*₆) δ 173.2, 132.8, 129.9, 125.8, 125.6, 68.8, 53.2, 52.7, 45.2, 37.1, 31.2, 19.9, 18.3; HRMS (ESI-TOF)⁺ (*m/z*) calcd for C₃₂H₄₃N₅O₄ (M + H⁺) 562.3294, found 562.3298. Anal. calcd for C₃₂H₄₃N₅O₄·H₂O: C, 66.3; H, 7.8; N, 12.0. Found: C, 66.3; H, 7.7; N, 12.2.

Synthesis of 16. To a clear solution of the *N*-hydroxysuccinimide ester of *N*-Cbz-*l*-phenyl **15** (30.0 g, 86.12 mmol) in anhydrous DME (250 mL) at 0 °C, diethylenetriamine (4.46 g, 43.06 mmol) dissolved in dry DME (20 mL) was added in a dropwise manner. The reaction mixture was stirred at room temperature for 18 h and then was heated to 40–50 °C for 6 h. The white solid was filtered and washed with cold distilled water and cold methanol to obtain a white solid (26.63 g, 40.05 mmol, yield 93%): mp 172–173 °C; IR (ATR): 3304, 1685, 1654, 1531, 1496, 1455 cm⁻¹; ¹H NMR (500 MHz, DMSO-*d*₆) δ 7.91 (s, 2H), 7.47 (d, 2H, *J* = 8.2 Hz), 7.12–7.37 (m, 20H), 4.95 (m, 4H), 4.22 (m, 2H), 3.12 (m, 4H), 2.98 (dd, 2H, *J* = 4.2 Hz; *J* = 13.3 Hz), 2.77 (dd, 2H, *J* = 10.2 Hz; *J* = 12.9 Hz), 2.58 (s, 4H); ¹³C NMR (125 MHz, DMSO-*d*₆) δ 172.8, 171.2, 155.8, 138.0, 136.9, 129.2, 128.2, 127.9, 127.6, 127.4, 126.2, 65.2, 56.2, 48.0, 37.7, 25.2; HRMS (ESI-TOF)⁺ (*m/z*) calcd for C₃₈H₄₃N₅O₆ (M + H⁺) 666.3292, found 666.3301. Anal. calcd for C₃₈H₄₃N₅O₆·H₂O: C, 66.7; H, 6.6; N, 10.2. Found: C, 66.5; H, 6.8; N, 10.2.

Synthesis of 17. To a stirred mixture of **16** (10.0 g, 15.0 mmol) and anhydrous K₂CO₃ in dry DMF (25 mL), methyl-2-bromoacetate (3.44 g, 22.5 mmol) was added and the reaction mixture was stirred at 50 °C for 24 h. The reaction progress was followed by TLC. After complete consumption of the starting material, distilled cold water (120 mL) was added and the reaction mixture extracted with EtOAc (75 mL, ×3). The organic phases were dried over anhydrous MgSO₄, and the solvent was evaporated under vacuum. The crude product was purified by silica flash chromatography using MeOH–CH₂Cl₂ (1 : 40) as the eluent to yield the white solid compound (8.40 g, 11.40 mmol, 76% yield): mp 156–158 °C; [α]_D²⁵ = –16.84° (*c* 0.1, CHCl₃); IR (ATR) 3305, 1698, 1685, 1643, 1533, 1455 cm⁻¹; ¹H-NMR (500 MHz, DMSO-*d*₆) δ 7.87 (s, 2H), 7.45 (d, 2H, *J* = 8.7 Hz), 7.11–7.36 (m, 20H), 4.97 (d, 2H, *J* = 12.7 Hz), 4.92 (d, 2H, *J* = 12.8 Hz), 4.23 (m, 2H), 3.61 (s, 3H), 3.40 (s, 2H), 3.12 (m, 4H), 2.99 (dd, 2H, *J* = 4.4 Hz; 13.9 Hz), 2.77 (dd, 2H, *J* = 10.4 Hz; 13.4 Hz), 2.61 (m, 4H); ¹³C-NMR (125 MHz, CDCl₃) δ 172.0, 171.9, 156.3, 137.1, 136.3, 129.3, 128.4, 127.8, 127.7, 126.6, 66.7, 56.4, 53.9, 53.4, 51.4, 38.3, 37.6; HRMS (ESI-TOF)⁺

(m/z) calcd for $C_{41}H_{47}N_5O_8$ ($M + H^+$) 738.3503, found 738.3505 ($M + H^+$). Anal. calcd for $C_{41}H_{47}N_5O_8$: C, 66.7; H, 6.4; N, 9.5. Found: C, 66.9; H, 6.7; N, 9.5.

Synthesis of 18. To a stirred clear solution of **17** (1.0 g, 1.4 mmol) in dry THF, 10 mol% of the catalyst (5 wt% Pd on activated carbon) was added. The reaction mixture was stirred under H_2 pressure (H_2 balloon) at 50 °C for 4 h. The reaction was monitored by using TLC. After complete consumption of the starting material the catalyst was filtered off through Celite® and washed with dry THF. The crude product was purified by silica flash chromatography using MeOH– CH_2Cl_2 (1 : 15) as an eluent, to which 20 μ L NH_3 were also added at every addition of the eluent throughout the column purification to give the sticky greenish oil **18** (0.401 g, 0.854 mmol, 61% yield): $[\alpha]_D^{25} = -48.14^\circ$ (c 0.1, $CHCl_3$); IR (ATR) 3296, 3086, 3026, 2946, 2848, 1734, 1644, 1521, 1454 cm^{-1} ; 1H NMR (500 MHz, DMSO- d_6) δ 7.80 (s, 2H), 7.26 (m, 4H), 7.20 (m, 6H), 3.60 (s, 3H), 3.37 (m, 4H), 3.09 (m, 4H), 2.93 (m, 2H), 2.55–2.66 (m, 6H), 1.90 (s, 2H); ^{13}C NMR (75 MHz, DMSO- d_6) δ 173.9, 171.6, 138.7, 129.5, 128.3, 127.7, 126.4, 125.7, 56.3, 54.4, 53.04, 50.9, 40.94, 36.9; HRMS (ESI-TOF) $^+$ (m/z) calcd for $C_{25}H_{35}N_5O_4$ ($M + H^+$) 470.2767, found 470.2760. Anal. calcd for $C_{25}H_{35}N_5O_4 \cdot 2H_2O$: C, 59.4; H, 7.8; N, 13.8. Found: C, 59.4; H, 7.7; N, 13.5.

Synthesis of 3. Compound **18** (0.80 g, 1.7 mmol), anhydrous K_2CO_3 (2.36 g, 17.0 mmol) and 9,10-bis-(bromomethyl)-anthracene (0.68 g, 1.7 mmol) were placed in a flask containing dry CH_3CN (150 mL) and the mixture was refluxed for 24 h under a nitrogen atmosphere. The reaction was filtered and the solvent evaporated under vacuum. The product was purified by flash silica chromatography using MeOH– CH_2Cl_2 (1 : 20) as an eluent to yield a yellow solid (0.708 g, 1.054 mmol, 62% yield): mp 77–78 °C; $[\alpha]_D^{25} = -171.34^\circ$ (c 0.1, $CHCl_3$); IR (ATR) 3335, 2943, 1734, 1657, 1509, 1437 cm^{-1} ; 1H NMR (500 MHz, CD_3CN) δ 8.39 (d, 2H, $J = 8.4$ Hz), 8.12 (d, 2H, $J = 8.4$ Hz), 7.50 (m, 4H), 7.43 (m, 4H), 7.36 (m, 6H), 6.68 (s, 2H), 4.63 (d, 2H, $J = 13.8$ Hz), 4.53 (d, 2H, $J = 13.8$ Hz), 3.55 (s, 3H), 3.47 (dd, 2H, $J = 9.1$ Hz; $J = 4.6$ Hz), 3.18 (dd, 2H, $J = 13.9$ Hz; $J = 4.6$ Hz), 3.01 (s, 2H), 2.70 (dd, 2H, $J = 13.9$ Hz; $J = 9.1$ Hz), 2.56 (m, 2H), 2.14–2.21 (m, 2H), 2.01–2.09 (m, 2H), 1.89–1.95 (m, 2H); ^{13}C NMR (500 MHz, CD_3CN) δ 173.1, 171.5, 138.4, 131.9, 129.8, 129.8, 129.4, 128.6, 126.7, 125.6, 125.5, 125.1, 125.0, 64.1, 52.8, 51.6, 50.7, 44.5, 39.0, 37.2; HRMS (ESI-TOF) $^+$ (m/z) calcd for $C_{41}H_{45}N_5O_4$ ($M + H^+$) 672.3550, found 672.3555. Anal. calcd for $C_{41}H_{45}N_5O_4$: C, 73.3; H, 6.8; N, 10.4. Found: C, 73.0; H, 6.9; N, 10.2.

Synthesis of 4. To a clear solution of **3** (0.58 g, 0.9 mmol) in 7 mL of THF– H_2O (2 : 1), LiOH was added (0.15 g, 6.3 mmol) and the reaction was stirred at room temperature for 24 h. The reaction was monitored by using TLC and, after complete consumption of the starting material, the reaction mixture was made acidic (pH 6) with 1 : 1 HBr– H_2O . To this solution, washed DOWEX® ion exchange resin (4 g) was added and the mixture was left for 18 h at room temperature. Then, the solvent of this mixture was evaporated under vacuum. The resulting solid was added to a column containing 20 g washed

DOWEX® ion exchange resin and deionized H_2O . The eluents used for the resin column purification were: 100 mL H_2O , 1 : 1 THF– H_2O 100 mL, 5% NH_3 in H_2O and then, 10% NH_3 in H_2O . From this resin column purification the compound was isolated in the range of 5–10% NH_3 in H_2O solutions. Then the water was evaporated under vacuum to yield the yellowish solid **4** (0.124 g, 0.189 mmol, 21% yield): mp 107–110 °C; $[\alpha]_D^{25} = -47.15^\circ$ (c 0.1, $CHCl_3$); IR (ATR) 3269, 3027, 1669, 1539 cm^{-1} ; 1H NMR (500 MHz, DMSO- d_6) δ 8.34 (d, $J = 8.6$ Hz, 2H), 8.18 (d, $J = 9.4$ Hz, 2H), 7.51 (m, 4H), 7.37 (s, 8H), 7.29 (s, 2H), 6.84 (s, 2H), 4.54 (m, 4H), 3.10 (m, 2H), 2.80 (s, 2H), 2.67 (dd, $J = 13.5$, 9.3 Hz, 3H), 2.08 (m, 4H), 1.87 (m, 2H); ^{13}C NMR (125 MHz, DMSO- d_6) δ 173.2, 139.1, 132.4, 129.9, 129.8, 128.8, 126.9, 125.8, 125.7, 125.4, 64.05, 53.2, 44.6, 39.1, 37.5; HRMS (ESI-TOF) $^+$ (m/z) calcd for $C_{40}H_{43}N_5O_4$ ($M + H^+$) 658.3393, found 658.3397 ($M + H^+$). Anal. calcd for $C_{40}H_{43}N_5O_4 \cdot H_2O$: C, 71.1; H, 6.7; N, 10.4. Found: C, 71.0; H, 6.9; N, 10.2.

Acknowledgements

Financial support from the Spanish MINECO (CTQ2012-38543-C03-01) and UJI (project P1-1B-2012-41) are acknowledged. P.D.W. thanks the financial support from GV (Grisolia Fellowship). M.J.M. acknowledges the School of Chemistry (University of East Anglia, Norwich, UK) for a studentship. The authors are grateful to Dr Jelena Gavrilovic (School of Biological Sciences, University of East Anglia, Norwich, UK) for the kind gift of the RAW 264.7 mouse macrophage cells used in this work.

Notes and references

- 1 D. Stephens, *Cell Imaging*, Scion Publishing, Oxfordshire, 1st edn, 2006.
- 2 M. Schäferling, *Angew. Chem., Int. Ed.*, 2012, **51**, 3532.
- 3 S. Yao and K. D. Belfield, *Eur. J. Org. Chem.*, 2012, 3199.
- 4 A. P. de Silva, H. Q. N. Gunaratne, T. Gunnlaugsson, A. J. M. Huxley, C. P. McCoy, J. T. Rademacher and T. E. Rice, *Chem. Rev.*, 1997, **97**, 1515.
- 5 S. Wang, N. Li, W. Pan and B. Tang, *Trends Anal. Chem.*, 2012, **39**, 3.
- 6 R. Freeman and I. Willner, *Chem. Soc. Rev.*, 2012, **41**, 4067.
- 7 Y. Yang, Q. Zhao, W. Feng and F. Li, *Chem. Rev.*, 2013, **113**, 192.
- 8 M. Y. Berezin and S. Achilefu, *Chem. Rev.*, 2010, **110**, 2641.
- 9 A. Thibon and V. C. Pierre, *Anal. Bioanal. Chem.*, 2009, **394**, 107.
- 10 J. R. Casey, S. Grinstein and J. Orlowski, *Nat. Rev. Mol. Cell Biol.*, 2010, **11**, 50.
- 11 F. J. Gennari, H. J. Adrogo, J. H. Galla and N. Maddius, *Acid-Base disorders and their treatment*, Taylor and Francis, Boca Raton, 2005.
- 12 A. H. Futerman and G. van Meer, *Nat. Rev. Mol. Cell Biol.*, 2004, **5**, 554.

- 13 C. Thivierge, J. Han, R. M. Jenkins and K. Burgess, *J. Org. Chem.*, 2011, **76**, 5219.
- 14 J. Han and K. Burgess, *Chem. Rev.*, 2010, **110**, 2709.
- 15 J. Han, A. Loudet, R. Barhoumi, R. C. Burghardt and K. Burgess, *J. Am. Chem. Soc.*, 2009, **131**, 1642.
- 16 R. Tang, H. Lee and S. Achilefu, *J. Am. Chem. Soc.*, 2012, **134**, 4545.
- 17 X. D. Wang, J. A. Stolwijk, T. Lang, M. Sperber, R. J. Meier, J. Wegener and O. S. Wolfbeis, *J. Am. Chem. Soc.*, 2012, **134**, 17011.
- 18 A. Grover, B. F. Schmidt, R. D. Salter, S. C. Watkins, A. S. Waggoner and M. P. Bruchez, *Angew. Chem., Int. Ed.*, 2012, **51**, 4838.
- 19 W. C. Sun, K. R. Gee, D. H. Klaubert and R. P. Haugland, *J. Org. Chem.*, 1997, **62**, 6469.
- 20 F.-Y. Ge and L.-G. Chen, *J. Fluoresc.*, 2008, **18**, 741.
- 21 A. P. de Silva and R. A. D. D. Rupasinghe, *J. Chem. Soc., Chem. Commun.*, 1985, 1669.
- 22 A. P. de Silva, H. Q. N. Gunaratne and C. P. McCoy, *Chem. Commun.*, 1996, 2399.
- 23 A. P. de Silva, T. Gunnlaugsson and T. E. Rice, *Analyst*, 1996, **121**, 1759.
- 24 A. P. de Silva, S. S. K. de Silva, N. C. W. Goonesekera, H. Q. N. Gunaratne, P. L. M. Lynch, K. R. Nesbitt, S. T. Patuwathavithana and N. L. D. S. Ramyalal, *J. Am. Chem. Soc.*, 2007, **129**, 3050.
- 25 S. Uchiyama, K. Iwai and A. P. de Silva, *Angew. Chem., Int. Ed.*, 2008, **47**, 4667.
- 26 R. A. Bissell, E. Calle, A. P. de Silva, S. A. de Silva, H. Q. N. Gunaratne, J.-L. Habib-Jiwan, S. L. A. Peiris, R. A. D. D. Rupasinghe, T. K. S. D. Samarasinghe, K. R. A. S. Sandanayake and J.-P. Soumillion, *J. Chem. Soc., Perkin Trans. 2*, 1992, 1559.
- 27 F. Galindo, M. I. Burguete, L. Vigara, S. V. Luis, N. Kabir, J. Gavrilovic and D. A. Russell, *Angew. Chem., Int. Ed.*, 2005, **44**, 6504.
- 28 M. I. Burguete, F. Galindo, M. Izquierdo, J. O'Connor, G. Herrera, S. V. Luis and L. Vigara, *Eur. J. Org. Chem.*, 2010, 5967.
- 29 E. Ko, J. Liu and K. Burgess, *Chem. Soc. Rev.*, 2011, **40**, 4411.
- 30 J. Becerril, M. Bolte, M. I. Burguete, F. Galindo, E. García-España, S. V. Luis and J. F. Miravet, *J. Am. Chem. Soc.*, 2003, **125**, 6677.
- 31 V. Marti-Centelles, M. I. Burguete and S. V. Luis, *Chem.-Eur. J.*, 2012, **18**, 2409.
- 32 G. Guillena, G. Rodríguez, M. Albrecht and G. Van Koten, *Chem.-Eur. J.*, 2002, **8**, 5368.
- 33 R. A. Bissell, A. P. de Silva, W. T. M. L. Fernando, S. T. Patuwathavithana and T. K. S. D. Samarasinghe, *Tetrahedron Lett.*, 1991, **32**, 425.
- 34 M. I. Burguete, F. Galindo, M. A. Izquierdo, S. V. Luis and L. Vigara, *Tetrahedron*, 2007, **63**, 9493.
- 35 G. J. Brown, A. P. de Silva, M. R. James, B. O. F. McKinney, D. A. Pears and S. M. Weir, *Tetrahedron*, 2008, **64**, 8301.
- 36 H. J. Lin, H. Szmazinski and J. R. Lakowicz, *Anal. Biochem.*, 1999, **269**, 162.
- 37 C. R. Schröder, B. M. Weidgans and I. Klimant, *Analyst*, 2005, **130**, 907.
- 38 Y. Urano, M. Kamiya, K. Kanda, T. Ueno, K. Hirose and T. Nagano, *J. Am. Chem. Soc.*, 2005, **127**, 4888.
- 39 L. F. Mottram, S. Boonyarattanakalin, R. E. Kovel and B. R. Peterson, *Org. Lett.*, 2006, **8**, 581.
- 40 M. Baruah, W. W. Qin, N. Basaric, W. M. De Borggraeve and N. Boens, *J. Org. Chem.*, 2005, **70**, 4152.
- 41 B. Tang, F. Yu, P. Li, L. L. Tong, X. Duan, T. Xie and X. Wang, *J. Am. Chem. Soc.*, 2009, **131**, 3016.
- 42 A. Bencini, A. Bianchi, E. Garcia-Espana, M. Micheloni and J. A. Ramirez, *Coord. Chem. Rev.*, 1999, **188**, 97.
- 43 J. F. Callan, S. Kamila, N. Singh, R. C. Mulrooney, M. Mackay, M. C. Cronin, J. Dunn and D. G. Durham, *Supramol. Chem.*, 2009, **21**, 643.
- 44 D. Soulet, B. Gagnon, S. Rivest, M. Audette and R. Poulin, *J. Biol. Chem.*, 2004, **279**, 49355.
- 45 M. J. Marín, P. Thomas, V. Fabregat, S. V. Luis, D. A. Russell and F. Galindo, *ChemBioChem*, 2011, **12**, 2471.
- 46 M. J. Marín, F. Galindo, P. Thomas and D. A. Russell, *Angew. Chem., Int. Ed.*, 2012, **51**, 9657.
- 47 M. J. Marín, F. Galindo, P. Thomas, T. Wileman and D. A. Russell, *Anal. Bioanal. Chem.*, 2013, **405**, 6197.